Quantifying pH-induced changes in plasma strong ion difference during experimental acidosis: clinical implications for base excess interpretation

Lorenzo Giosa[1,2]; Francesco Zadek[3]; Mattia Busana[4]; Giovanna De Simone[5]; Serena Brusatori[6]; Martin Krbec[7]; Frantisek Duska[7]; Paolo Brambilla[3]; Alberto Zanella[6]; Alessandra Di Masi[5]; Pietro Caironi[8]; Emanuele Perez[9]; Luciano Gattinoni[4]; Thomas Langer[3,10]

[1] Department of Critical Care Medicine, Guy's and St. Thomas' National Health Service Foundation Trust, London, UK. [2] Centre for Human and Applied Physiological Sciences, King's College London, London, UK. [3]Department of Medicine and Surgery, University of Milano-Bicocca, Monza, Italy. [4]Department of Anesthesiology, University Medical Center Göttingen, Göttingen, Germany. [5]Department of Sciences, Roma Tre University, Rome, Italy. [6]Department of pathophysiology and Transplantation, University of Milan, Milan, Italy. [7]Department of Anesthesia and Intensive Care Medicine, The Third Faculty of Medicine, Charles University and FNKV University Hospital, Prague, Czechia [8]Department of Anesthesia and Critical Care, AOU S. Luigi Gonzaga; Department of Oncology, University of Turin, Turin, Italy. [9]Department of biomedical and neuromotor sciences, Headquarter of Human physiology, University of Bologna, Bologna, Italy. [10]Department of Anesthesia and Intensive Care Medicine, Niguarda Ca' Granda, Milan, Italy.

CORRESPONDING AUTHOR

Thomas Langer, MD; Department of Medicine and Surgery, University of Milan-Bicocca, Monza, Italy; Department of Anesthesia and Intensive Care Medicine, Niguarda Ca' Granda, Milan, Italy, Italy. Tel. +39 02 64448580; email: Thomas.Langer@unimib.it

RUNNING HEAD

Relationship between base excess and strong ion difference

ABSTRACT

It is commonly assumed that changes in plasma strong ion difference (SID) result in equal changes in whole-blood base excess (BE). However, at varying pH, albumin ionic-binding and transerythrocyte shifts alter the SID of plasma without affecting that of whole-blood (SID_{wb}), *i.e.*, the BE. We hypothesize that, during acidosis, 1) an *expected* plasma SID (SID_{exp}) reflecting electrolytes redistribution can be predicted from albumin and hemoglobin's charges, and 2) only deviations in SID from SID_{exp} reflect changes in SID_{wb}, and therefore, BE. We equilibrated whole-blood of 18 healthy subjects (albumin=4.8±0.2 g/dL, hemoglobin=14.2±0.9 g/dL), 18 hypoalbuminemic and anemic septic patients (albumin=3.1±0.5 g/dL, hemoglobin=10.4±0.8 g/dL), and 10 healthy subjects after in-vitro induced isolated anemia (albumin=5.0±0.2 g/dL, hemoglobin=7.0±0.9 g/dL) with varying CO_2 concentrations (2-20%). Plasma SID increased by 12.7±2.1, 9.3±1.7, and 7.8±1.6 mEq/L, respectively ($p<0.01$) and its agreement (bias[limits of agreement]) with SID_{exp} was strong: 0.5[-1.9;2.8], 0.9[-0.9;2.6], and 0.3[-1.4;2.1] mEq/L, respectively. Separately, we added 7.5 or 15 mEq/L of lactic or hydrochloric acid to whole-blood of 10 healthy subjects obtaining BE of -6.6±1.7, -13.4±2.2, -6.8±1.8, and -13.6±2.1 mEq/L, respectively. The agreement between ΔBE and ΔSID was weak (2.6[-1.1;6.3] mEq/L), worsening with varying CO_2 (2-20%): 6.3[-2.7;15.2] mEq/L. Conversely, ΔSID_{wb} (the deviation of SID from SID_{exp}) agreed strongly with ΔBE at both constant and varying CO_2: -0.1[-2.0;1.7], and -0.5[-2.4;1.5] mEq/L, respectively. We conclude that BE reflects only changes in plasma SID that are not expected from electrolytes redistribution, the latter being predictable from albumin and hemoglobin's charges.

NEW & NOTEWORTHY

This paper challenges the assumed equivalence between changes in plasma strong ion difference (SID) and whole-blood base excess (BE) during in-vitro acidosis. We highlight that redistribution of strong ions, in the form of albumin ionic-binding and transerythrocyte shifts, alters SID without affecting BE. We demonstrate that these *expected* SID alterations are predictable from albumin and hemoglobin's charges, or from the non-carbonic whole-blood buffer value, allowing a better interpretation of SID and BE during in-vitro acidosis.

KEYWORDS

Whole-blood base excess; Plasma strong ion difference; Albumin; Hemoglobin, Non-carbonic whole-blood buffer value.

INTRODUCTION

Whole-blood base excess (BE) is the PCO_2-independent variable that quantitatively describes metabolic acidosis in-vitro (1). It is calculated as the deviation of buffer base (BB) from its normal value (2). The buffer base represents the total negative charge on blood buffers, namely bicarbonate, proteins and phosphate species (3).

Under all circumstances, the negative charge of the buffer base is balanced by an equal and positive strong ion difference (SID), *i.e.*, the difference between strong cations (mainly Na^+, K^+, Ca^{2+} and Mg^{2+}) and anions (mainly Cl^-, Lac^- and unmeasured anions).

For electroneutrality to be preserved, when SID deviates from its normal value (*e.g.*, for addition of strong ions to blood), the buffer base must change of an equal amount (3).

Accordingly, in solutions with constant concentration of total weak acids, the following statement holds true: *since* $\mathrm{BE} = \Delta\mathrm{BB}$ *and* $\Delta\mathrm{SID} = \Delta\mathrm{BB}$, *then* $\Delta\mathrm{SID} = \mathrm{BE}$. Briefly, any change in strong ion difference should be reflected by an equal base excess. For instance, in a patient with hyperchloremia where SID decreases by 10 mEq/L, BE should decrease by 10 mEq/L. This assumption is now part of several acid-base models attempting to partition the base excess at the bedside (4–9). However, this approach has been largely criticized, in that it represents an inappropriate application of the Stewart's *plasma* acid-base model to the *whole-blood* concept of BE (10, 11). Indeed, according to Stewart, SID is independent of pH, and rather determines pH when deviating from normal (12). However, the SID that is measured in *plasma* is not pH-independent in *whole-blood*: the plasma concentration of strong ions changes at varying pH, due to binding of electrolytes to albumin (13–15) and, more importantly, to shifts of electrolytes and water between plasma and red cells (16, 17). This physiological redistribution of strong ions does not alter the total pool of blood charges (*i.e.*, the SID of whole-blood), and thereby should not affect

BE. For instance, when CO_2 increases in blood, the reducing pH forces water and chloride into the red cells, thereby increasing plasma SID (18, 19). However, BE does not concomitantly change, as electrolytes do not physically leave blood (the whole-blood SID remains constant), but simply change compartment (20). Similarly, during metabolic acidosis, addition of acid to blood reduces BE by an equal amount (*e.g.*, addition of 10 mEq/L of lactic acid reduces BE by 10 mEq/L), but the total reduction in plasma SID is lower, as some chloride, lactate and water are forced into the red cells by the decreasing pH (21–23).

Although these concepts have been largely explored in the past, a quantification of the *expected* changes in plasma SID at varying pH is lacking, and it is unknown how this may influence the relationship between plasma SID and whole-blood BE.

The aim of this in-vitro study is therefore two-fold: *first*, to simplify the quantification of electrolytes/water redistribution at varying pH, currently prerogative of complex computerized acid-base models (11, 24). Here, we hypothesize that this phenomenon can be modeled as a simple function of the titrable (pH-dependent) charge on albumin and hemoglobin (25), the predominant non-carbonic buffers in blood (26) (**Figure 1**). On these grounds, we will introduce the novel concept of *expected* strong ion difference (SID_{exp}), defined as the predictable plasma SID that is expected to result from electrolytes redistribution at varying pH. *Second*, we aim to compare changes in SID and BE during metabolic and mixed acidosis. We hypothesize that only changes in plasma SID that are not explained by *expected* electrolytes and water shifts will reflect changes in *whole-blood* SID, and thereby be paralleled by an equal BE.

METHODS

Study populations

We tested our hypotheses in three *in-vitro* experiments investigating:

1) Respiratory acidosis in isolated plasma and whole-blood of 18 healthy subjects and 18 age-matched septic patients with anemia and hypoalbuminemia (18);
2) Respiratory acidosis in whole-blood of 10 healthy subjects before and after in-vitro induced isolated anemia;
3) Respiratory, metabolic, and mixed acidosis in whole-blood of 10 healthy subjects (27).

Detailed methods for Experiments 1 and 3 were previously published elsewhere (18, 27). All experiments were approved by the local ethical committee (Comitato Etico Milano Area 2, Protocol 124_2018bis).

Procedures and measurements

Experiment 1

A venous blood sample was assessed for hemoglobin, albumin, phosphate and magnesium concentrations (Cobas c-702, Roche, Switzerland). Isolated plasma was then separated from whole-blood by centrifugation. Subsequently, plasma and whole-blood samples were equilibrated (Equilibrator, RNA Medical) with heated (37°C) and oxygenated (21% O_2) gas mixtures containing four CO_2 concentrations (2, 5, 12 and 20%). Blood gases and electrolytes were assessed at every equilibrated CO_2 (ABL 800 FLEX Radiometer, Denmark). Further details are available at (18).

Experiment 2

Venous blood was collected with a vacuum technique in lithium-heparin tubes (Vacuette® Plasma Lithium Heparin 4mL Tubes, Greiner Bio-One™, Kremsmünster, AT). Each subject provided six tubes, of which one was used for pre-protocol analyses, one was used as “non-diluted” sample, and three underwent centrifugation at 4°C at 3000 rpm for 12 minutes to obtain isolated plasma. Plasma was then mixed with whole-blood in the remaining tube, obtaining a “diluted” sample with anemia (half the initial hematocrit) and normoalbuminemia. Diluted and non-diluted whole-blood samples were assessed for hemoglobin, albumin, phosphate and magnesium concentrations (Cobas c-702, Roche, Switzerland), then equilibrated (Equilibrator, RNA Medical) with heated (37°C) and oxygenated (21% O_2) gas mixtures containing three CO_2 concentrations (2, 12 and 20%). Blood gases and electrolytes were measured at every equilibrated CO_2 (ABL 800 FLEX Radiometer, Denmark).

Experiment 3

A venous blood sample was assessed for blood count, albumin, phosphate and magnesium concentrations (Cobas c-702, Roche, Switzerland), then mixed with five stock electrolytes solutions to obtain:

- A control sample (SID similar to normal plasma: “Ctr”);
- Two samples with hyperchloremic acidosis (addition of ~ 7.5 and 15 mEq/L of hydrochloric acid: “Cl 7.5” and “Cl 15”);
- Two samples with lactic acidosis (addition of ~ 7.5 and 15 mEq/L of lactic acid: “Lac 7.5” and “Lac 15”).

After mixing, all samples were equilibrated (Equilibrator, RNA Medical) with heated (37°C) and oxygenated (21% O_2) gas mixtures containing ~10 different CO_2 concentrations (from

2 to 20%), then assessed for blood gases and electrolytes (ABL 90 Radiometer, Denmark). Further details are available at (27).

Baseline

In every experiment, a baseline step was defined as the one with pH closest to 7.4 and PCO_2 closest to 40 mmHg. Specifically:

1) Experiment 1: samples equilibrated with 5% CO_2
2) Experiment 2: samples equilibrated with 12% CO_2
3) Experiment 3: the control samples (Ctr) with PCO_2 closest to 40 mmHg.

Changes in measured and calculated variables from baseline will be referred to as Δ throughout the manuscript.

Calculations

Variables calculated in all experiments

SID was calculated from measured plasma electrolytes as:

Equation 1

$$\mathrm{SID} = [\mathrm{Na^+}] + [\mathrm{K^+}] + [\mathrm{Ca^{2+}}] + [\mathrm{Mg^{2+}}] - [\mathrm{Cl^-}] - [\mathrm{Lac^-}].$$

Where brackets indicate concentrations (mEq/L) of sodium (Na^+), potassium (K^+), ionized calcium (Ca^{2+}), magnesium (Mg^{2+}), chloride (Cl^-) and lactate (Lac^-). Magnesium concentration was available at baseline only and was considered constant throughout the experiments.

Albumin and hemoglobin's titrable charges (Z_{pH}) in mEq/L were computed from Watson (25) as:

Equation 2

$$Z_{pH} = c \cdot \frac{n \cdot 10^{-pH}}{10^{-6.75} + 10^{-pH}}$$

where *c* is the concentration of the protein in mMol/L, pH refers to plasma for albumin and red cells for hemoglobin (16), *n* is the number of titrable groups on each protein (27,28), and 6.75 is their average dissociation constant (30) (see **Supplemental Material**, https://doi.org/10.6084/m9.figshare.24903429.v1, **Figure S1**, https://doi.org/10.6084/m9.figshare.24903384, and **Figure S2**, https://doi.org/10.6084/m9.figshare.24903414).

The expected SID (SID_{exp}) was calculated as:

Equation 3

$$SID_{exp} = SID_{(baseline)} + \Delta Z_{pH}$$

Where Z_{pH} refers to albumin in isolated plasma, and to albumin + hemoglobin in whole-blood.

Additional variables calculated in Experiment 3

Participants specific non-carbonic whole-blood buffer values (β) were obtained as the opposite of the first derivative of the HCO_3^-/pH curve during CO_2 tonometry as previously described (27):

Equation 4

$$\beta = -\frac{d[HCO_3^-]}{dpH}$$

An alternative expected SID derived from β ($SID_{exp(\beta)}$) was calculated as:

Equation 5

$$\mathrm{SID}_{\exp(\beta)} = \mathrm{SID}_{(\mathrm{baseline})} - \beta \cdot (\mathrm{pH} - \mathrm{pH}_{(\mathrm{baseline})})$$

Whole-blood BE was computed with Zander's equation (31) using participants' specific β values (27):

Equation 6

$$\mathrm{BE} = \mathrm{r} \cdot [(\mathrm{HCO_3^-} - 24.26) + \beta \cdot (\mathrm{pH} - 7.4)] - \mathrm{s}$$

Where *r* is the distribution ratio of bicarbonate, calculated as 1 – 0.0143· [Hb] ([Hb] being hemoglobin concentration in g/dL), while *s* represents the effect of hemoglobin saturation on BE, and is calculated as 0.2·[Hb]·(1 – sO_2), with sO_2 being the fraction of saturated hemoglobin.

Changes in whole-blood SID (ΔSID_{wb}) were calculated as:

Equation 7

$$\Delta\mathrm{SID}_{\mathrm{wb}} = \mathrm{r} \cdot (\mathrm{SID} - \mathrm{SID}_{\exp(\beta)})$$

<u>Simplified model</u>

A simplified model was built using calculations recommended by the Clinical and Laboratory Standards Institute (CLSI) (32) and available in current blood gas analyzers. Specifically, in all experiments we calculated the buffer value of whole-blood as:

Equation 8

$$\beta_{\mathrm{CLSI}} = 1.43 \cdot [\mathrm{Hb}] + 7.7$$

We then used β_{CLSI} to calculate an expected SID ($SID_{exp(CLSI)}$) as:

Equation 9

$$\mathrm{SID}_{\mathrm{exp(CLSI)}} = \mathrm{SID}_{\mathrm{(baseline)}} - \beta_{\mathrm{CLSI}} \cdot (\mathrm{pH} - \mathrm{pH}_{\mathrm{(baseline)}})$$

Analogous to Equations 6 and 7, In Experiment 3 we also calculated whole-blood base excess and changes in whole-blood SID using CLSI standards:

Equation 10

$$\mathrm{BE}_{\mathrm{CLSI}} = \mathrm{r} \cdot [(\mathrm{HCO}_3^- — 24.26) + \beta_{\mathrm{CLSI}} \cdot (\mathrm{pH} - 7.4)]$$

Equation 11

$$\Delta\mathrm{SID}_{\mathrm{wb(CLSI)}} = \mathrm{r} \cdot (\mathrm{SID} - \mathrm{SID}_{\mathrm{exp(CLSI)}})$$

Statistical analysis

All data are reported as mean ± standard deviation (SD). Normality of distributions was assessed with histograms and QQ plots. In all experiments, Bland-Altman analysis was employed to describe the agreement (expressed as mean bias [limits of agreement]) between SID and SID_{exp}, and SID and $SID_{exp(CLSI)}$ at varying CO_2. In Experiment 3 we also assessed the agreement between SID and $SID_{exp(\beta)}$, ΔBE and ΔSID, ΔBE and ΔSID_{wb}, ΔBE_{CLSI} and ΔSID, and ΔBE_{CLSI} and $\Delta SID_{wb(CLSI)}$. Agreements were considered clinically acceptable if bias was within ± 1 mEq/L and maximal difference < 3 mEq/L (33). Between groups differences (*e.g.*, Healthy subjects vs Septic patients in Experiment 1) were assessed with Student's t-test. Pearson's r coefficient was used to describe associations

245 between variables. Two-tailed $p < 0.05$ was considered statistically significant. The graphs
246 were formulated with SigmaPlot v.16.0. R-4.2.2 was used for statistical computing.

247

RESULTS

Experiment 1

Albumin and hemoglobin were higher in healthy subjects than in septic patients: 4.8±0.2 vs 3.1±0.5 g/dL and 14.2±0.9 vs 10.4±0.8 g/dL, respectively (both $p<0.01$).

In isolated plasma, from 2 to 20% CO_2, the measured strong ion difference (SID) increased by 2.9 ± 1.0 mEq/L in healthy subjects, and 2.1 ± 0.7 mEq/L in septic patients ($p < 0.01$). The agreement with the predicted strong ion difference (SID_{exp}) was strong: 0.0 [-2.0;2.0] mEq/L and 0.4 [-1.6;2.4] mEq/L, respectively (**Figure 2-Panel A**).

In whole-blood (**Table 1**), from 2 to 20% CO_2, the measured plasma strong ion difference (SID) increased by 12.7 ± 2.1 mEq/L in healthy subjects, and 9.3 ± 1.7 mEq/L in septic patients ($p < 0.01$). The agreement with the predicted strong ion difference (SID_{exp}) was strong: 0.5 [-1.9;2.8] mEq/L and 0.9 [-0.9;2.6] mEq/L, respectively (**Figure 2-Panel B**).

Figure S3 (https://doi.org/10.6084/m9.figshare.24899334.v2) reports changes in single electrolytes during acidosis.

Experiment 2

Albumin was similar in diluted and non-diluted samples (5.0±0.2 vs 5.0±0.3 g/dL, $p>0.99$), while hemoglobin was significantly lower in the former (7.0±0.9 vs 14.1±1.7 g/dL, $p<0.01$).

As shown in **Table 2**, from 2 to 20% CO_2, the measured strong ion difference (SID) increased by 12.4 ± 2.0 mEq/L in non-diluted samples, and 7.8 ± 1.6 mEq/L in the diluted samples ($p <0.01$). The agreement with the predicted strong ion difference (SID_{exp}) was strong: 0.7 [-0.8;2.2] mEq/L and 0.3 [-1.4;2.1] mEq/L, respectively (**Figure 3**).

Experiment 3

Albumin and hemoglobin concentrations were 5.0±0.2 and 13.9±1.3 g/dL, respectively.

In the control sample (Ctr), from 2 to 20% CO_2 the measured strong ion difference (SID) increased by 12.3 ± 4.6 mEq/L. The agreement with the predicted strong ion difference was 0.2 [-1.9;2.3] mEq/L when using SID_{exp}, and 0.5 [-1.1;2.1] mEq/L when using $SID_{exp(\beta)}$ (**Figure 4**).

As shown in **Table 3**, when compared to baseline, samples with added lactate or chloride (Lac 7.5, Cl 7.5, Lac 15, Cl 15) and constant equilibrated CO_2 (pure metabolic acidosis) showed a decrease in BE of -6.6 ± 0.5, -6.8 ± 0.7, -13.4 ± 0.9, and -13.6 ± 1.0 mEq/L, respectively, while the concomitant decrease in SID was significantly lower: -5.4 ± 1.3, -4.9 ± 0.7, -10.2 ± 1.6, and -9.5 ± 1.2 mEq/L, respectively, all $p < 0.01$ (see **Figure S4**, https://doi.org/10.6084/m9.figshare.24899343.v2, for changes in single electrolytes). The agreement between ΔBE and ΔSID was weak: 2.6[-1.1;6.3] mEq/L. Conversely, the agreement between ΔBE and ΔSID_{wb} was strong: -0.1[-2.0;1.7] mEq/L (**Figure 5-Panel A**).

When comparing baseline with any other sample (Lac 7.5, Lac 15, Cl 7.5, Cl 15) at any equilibrated CO_2 from 2 to 20% (mixed acidosis) the overall agreement between ΔBE and ΔSID was very weak (6.3[-2.7;15.2] mEq/L), while between ΔBE and ΔSID_{wb} it remained strong: -0.5[-2.4;1.5] mEq/L (**Figure 5-Panel B**).

Simplified model

Results are presented in **Figure S5** (https://doi.org/10.6084/m9.figshare.24899337.v2): **Panels A-B** refer to all experiments during respiratory acidosis. The agreement between SID and $SID_{exp(CLSI)}$ was strong: 0.5 [-2.3;3.3] mEq/L, with only 16/258 comparisons (6.2%) showing a bias ≥ 3 mEq/L (**Panel A**). The bias was proportional to albumin's concentration ($p < 0.01$, Pearson's r 0.35, **Panel B**). **Panels C-D** refer to Experiment 3: during pure

metabolic acidosis (**Panel C**), the agreement between ΔBE_{CLSI} and ΔSID was weak (1.9 [-1.1;5.0] mEq/L), while between ΔBE_{CLSI} and $\Delta SID_{wb(CLSI)}$ it was strong: -0.1 [-1.9;1.7] mEq/L. During mixed acidosis (**Panel D**), the agreement between ΔBE_{CLSI} and ΔSID worsened (5.1 [-2.5;12.7] mEq/L), while between ΔBE_{CLSI} and $\Delta SID_{wb(CLSI)}$ it remained strong: -0.5 [-2.4;1.3] mEq/L.

DISCUSSION

The results of the present study can be divided into:

1. *Physiological findings*: changes in plasma SID due to redistribution of strong ions at varying pH can be predicted from albumin and hemoglobin's titrable charges, *i.e.*, from the non-carbonic buffer value of whole-blood.
2. *Clinical implication*: only changes in plasma SID that are not explained by redistribution of strong ions are paralleled by equal changes in BE.

Physiological findings

Isolated plasma

In 1992 Fogh-Andersen demonstrated that the total net charge on albumin was more negative than the charge of its lateral aminoacidic residues, due to an excess of bound chloride with respect to positive electrolytes. He also found that, at varying pH, changes in albumin's bound-electrolytes tended to preserve the total net charge on the protein by compensating for the change in its titrable charge Z_{pH} (14) (**Figure S1**, https://doi.org/10.6084/m9.figshare.24903384). Based on Fogh-Andersen's data, we hypothesized that pH-induced changes in SID in isolated plasma would be predictable from changes in albumin's Z_{pH}. The results of Experiment 1 corroborated this hypothesis in both healthy subjects and septic patients.

Of note, Fogh-Andersen's data predicted only changes in chloride and calcium at varying pH (**Figure 1**). Here, we also found changes in sodium (**Figure S3-Panel A**, https://doi.org/10.6084/m9.figshare.24899334.v2), as previously reported by others in similar experiments: Staempfli and Constable ascribed them to measurements artifacts

(34); others suggested instead that sodium-albumin binding and/or water-albumin binding at varying pH would be more reasonable explanations (35).

Whole-blood

The distribution of electrolytes between plasma and red blood-cells is a function of the electrical charge of compartmentalized molecules (essentially albumin and hemoglobin), as determined by the Donnan theory (36). Accordingly, in an isolated red blood-cells experiment, Dalmark found that changes in the intracellular concentration of chloride at varying pH were solely determined by hemoglobin's buffer value, *i.e*., by the change in its titrable charge (17). Combining the models of Fogh-Andersen (14) and Dalmark (17), we have demonstrated that the overall change in plasma SID during whole-blood CO_2 tonometry can be predicted from albumin and hemoglobin's titrable charges: in all our experiments, the agreement between the expected and measured SID was strong across a wide pH-range. Experiments 1 and 2 also showed that hypoalbuminemia and/or anemia are associated with lower changes in plasma SID at varying pH, further corroborating our hypothesis.

Confirmation of the major role of albumin and hemoglobin in driving electrolytes redistribution at varying pH can also be found in Reeves, pioneer of the alpha-stat theory (37). This author demonstrated that when blood's pH is altered by temperature variations no redistribution of electrolytes occurs (38), as imidazoles ionization remains unchanged (*i.e*., Z_{pH} is constant).

An intuitive explanation to the observed relationship between albumin and hemoglobin's titrable charges and electrolytes' redistribution can be given based on bicarbonate kinetics and the law of electroneutrality: briefly, albumin and hemoglobin are responsible either for the increase in plasma bicarbonate during *respiratory acidosis*, or for blunting its reduction during *metabolic acidosis* (39). As detailed below, under both circumstances, the

exceeding negative charge of bicarbonate must be balanced by an equal increase in plasma positive charges. This can only be obtained by a displacement of strong ions, increasing the SID.

Respiratory acidosis

Carbon dioxide equally diffuses in plasma and red cells, and it is mainly buffered by albumin and hemoglobin leading to an increase in bicarbonate (40). In isolated plasma, the negative charge of bicarbonate is initially balanced by an equal increase in the positive titrable charge (Z_{pH}) on albumin's imidazoles (3), which in turn drives an equal binding of electrolytes to preserve the total net charge on the protein as per Fogh-Andersen's model (14) (**Figure S1**, https://doi.org/10.6084/m9.figshare.24903384). This process is paralleled, in whole-blood, by an increase in erythrocytes' bicarbonate determined by hemoglobin's buffer value (26). The increasing red cells' bicarbonate then shifts to plasma where, for electroneutrality to be preserved, an equal increase is SID must occur. The latter is obtained through a shift of chloride and water into the erythrocytes, decreasing the plasma concentration of chloride and increasing that of cations (16) (**Figure S3-Panel B**, https://doi.org/10.6084/m9.figshare.24899334.v2). The overall effect of respiratory acidosis in whole-blood is therefore that $\Delta_{(plasma)}HCO_3^- = \Delta_{(Albumin)}Z_{pH} + \Delta_{(Hemoglobin)}Z_{pH} = \Delta_{(plasma)}SID$. This one-to-one increase in bicarbonate and SID at varying CO_2 was recently confirmed in vivo by our group (20).

Metabolic acidosis

Addition of lactate or chloride to blood is initially buffered in plasma by bicarbonate and, to a lesser extent, by albumin (39). As above, the increasing positive albumin's titrable charge (Z_{pH}) drives an equal binding of electrolytes following Fogh-Andersen's model (14). The CO_2 formed in plasma by the bicarbonate buffer system then shifts into red cells, where it regenerates bicarbonate in an amount that depends on hemoglobin's buffer value

(41, 42). The newly formed red cells' bicarbonate moves back to plasma where its increasing negative charge must be balanced by an equal increase in SID. This is obtained through a shift of chloride, water and of the added ion itself, if permeant, into the erythrocytes (**Figure S4**, https://doi.org/10.6084/m9.figshare.24899343.v2). The overall effect of metabolic acidosis in whole-blood is therefore that $\Delta_{(plasma)}Acid^- - \Delta_{(plasma)}HCO_3^- = \Delta_{(Albumin)}Z_{pH} + \Delta_{(Hemoglobin)}Z_{pH} = \Delta_{(plasma)}SID$.

Non carbonic whole-blood buffer value (β)

The titrable charge on albumin and hemoglobin (Z_{pH}) is not routinely calculated in clinical practice. However, these proteins are the main determinants of the non-carbonic buffer value of whole-blood (β) (26), and, in Experiment 3, we have shown that patient's specific β can be used to predict pH-induced changes in plasma SID with equivalent accuracy compared to Z_{pH}. Interestingly, the prediction remained clinically acceptable when using β_{CLSI} in our simplified model. This broadens the clinical applicability of our findings, as CLSI standards are currently used by bedside blood gas analyzers. As expected, the accuracy of the simplified model worsened with hypoalbuminemia (**Figure S5-Panel B**, https://doi.org/10.6084/m9.figshare.24899337.v2), as CLSI assumes normal values of plasma proteins. However, the bias remained largely acceptable from a clinical standpoint.

It can be concluded that pH-induced changes in plasma SID are a function of the non-carbonic whole-blood's buffer value, *i.e.*, of the change in albumin and hemoglobin's titrable charge at varying pH.

Clinical implications

The possibility of predicting changes in SID at varying pH finds a strong clinical implication in the interpretation of BE. Indeed, BE reflects changes in *whole-blood* SID (24), which

cannot be directly measured, but that our model allows to estimate indirectly with two simple steps: *first*, the difference between the measured and expected plasma SID reflects the amount of acid added to *plasma*; *second*, conversion to *whole-blood* is possible by means of the distribution ratio of bicarbonate (**Equation 7**). The assumption is that lactate and chloride, the most common measurable metabolic acids in clinical practice, distribute between plasma and red cells in the same manner as bicarbonate, as previously shown (43, 44). The validity of this model is demonstrated by Experiment 3, showing a very strong agreement between changes in BE and in our calculated *whole-blood* SID during both metabolic and mixed acidosis.

Conversely, changes in BE and plasma SID agreed very poorly, especially during mixed disturbances, where differences up to 15 mEq/L were observed. This corroborates the hypothesis that variations in the *plasma* concentrations of strong ions do not reflect changes in the net pool of *whole-blood* charges, and, thereby, should not be considered as proxy of BE. Our findings are at variance with current models attempting to partition BE into *plasma* components using the Fencl-Stewart approach (4–9): these models consider that any deviation in SID from a fixed, reference value (*e.g.*, 41.7 mEq/L(3)) is paralleled by an equal BE. On the contrary, we have demonstrated that part of the change in SID during acidosis reflects redistribution of electrolytes which does not alter the whole-blood SID, and thereby the BE. A practical example is given in **Figure 6**, where we applied our model and the Fencl-Stewart equation to whole blood of one of the healthy subjects from Experiment 3, with in-vitro induced mixed hypercapnic and hyperchloremic acidosis (pH 7.05, PCO_2 79.9 mmHg, $[Cl^-]$ 118 mEq/L). As shown, despite the hyperchloremia with reduced BE (-10 mEq/L), the plasma SID is almost normal (40.3 mEq/L). Since the concentration of total weak acids (albumin and phosphate) is also normal, the Fencl-Stewart equation concludes that unmeasured ions (UI) are present to explain the BE.

Conversely, our simplified model calculates a change in whole-blood SID of -9.3 mEq/L, confirming that the BE is entirely explained by SID variations. This is likely the reason why the Fencl-Stewart equation might be inaccurate in estimating UI when compared to the reference method, *i.e.*, the strong ion gap (33). It must be acknowledged, however, that the Fencl-Stewart approach is intended for a bedside evaluation of acid-base disturbances, and, despite its simplifying assumptions, it carries undoubtful clinical benefits in this regard (5). Moreover, as expanded in the “Limitations” section (see below), it uses the base excess of the extracellular fluid (4) rather than whole-blood base excess, and application of our in-vitro findings to the extracellular space requires validation.

Limitations

Some limitations must be highlighted: first, our model relies on the calculation of SID, which might be affected by measurements’ inaccuracies depending on the type of blood gas analyzer used (45). The fact that two different machines were used in this study (one for Experiment 1 and 2, and a different one for Experiment 3) with very similar results alleviates our concerns in this regard; *second*, magnesium concentration was only assessed at baseline and considered constant throughout the experiments: while we acknowledge that binding to albumin (15) and transerythrocyte movements of water might affect magnesium concentration at varying pH, we do not believe that this altered our results in a quantitatively significant manner; *third*, our model does not take into consideration phosphate species: both inorganic phosphate in plasma and 2,3 bisphosphoglycerate in red cells contribute to whole-blood buffering (26), and the former also freely moves between plasma and red-cells (46). However, the quantitative role of these species is small (26), and their concentration is hardly ever available in clinical practice. Accordingly, their inclusion in this model would reduce its clinical applicability

463 while only minimally improving its accuracy. This is demonstrated by the results relative to
464 $SID_{exp(\beta)}$ in **Figure 4**, where accounting for the contribution of phosphate species through
465 the whole-blood buffer value β did not significantly change our results; *finally*, our results
466 are limited by the in-vitro nature of the experiments, and in-vivo applicability remains to be
467 demonstrated. Importantly, the in-vivo PCO_2-independent parameter of acute metabolic
468 acidosis is the extracellular, or standard, base excess (SBE) rather than whole-blood BE
469 (20, 47). As the extracellular buffer value β is lower than whole-blood's (26), changes in
470 plasma SID at varying pH are expected to be lower in-vivo than in-vitro. Accordingly, we
471 have recently shown that pH-dependent changes in plasma SID during in-vivo acute
472 *respiratory* acidosis equal changes in plasma bicarbonate (20), which are a function of the
473 extracellular buffer value β. A significant redistribution of strong ions has also been
474 previously reported during in-vivo acute *metabolic* acidosis (21, 23). It is important to point
475 out that this study does not suggest using whole-blood BE rather than SBE in clinical
476 practice. However, the *in-vitro* nature of the experiments did not allow us to calculate SBE,
477 nor to validate our prediction of changes in plasma SID for *in-vivo* acidosis. This is
478 currently being investigated by our group as a future project.

479

CONCLUSIONS

During experimental acidosis, changes in plasma SID reflecting electrolytes redistribution can be predicted from concomitant changes in albumin and hemoglobin's titrable charges or, simpler, from the non-carbonic buffer value of whole-blood (β). *Expected* changes in SID can be used to assess the actual contribution of strong ions to base excess, allowing an accurate interpretation of this widely used indicator of metabolic acidosis. All variables used in this model are available in clinical practice, including β_{CLSI}, which is currently incorporated in blood gas analyzers for the calculation of BE (31). This is a great advantage with respect to previous comprehensive acid base models, which require complex calculations limiting clinical applicability (11, 24). Validation of our findings in-vivo might improve the bedside understanding of metabolic acidosis.

DATA AVAILABILITY

The complete dataset is available at https://doi.org/10.6084/m9.figshare.24903423

ACKNOWLEDGMENTS

None

GRANTS

None

DISCLOSURES

No conflicts of interest, financial or otherwise, are declared by the authors.

AUTHOR CONTRIBUTIONS

Lo.G., T.L., P.C., E.P., A.Z., F.D., and Lu.G. conceptualized the study. S.B., F.Z., M.K. and PB collected the data and performed the experiments. G.d.S. and A.d.M. provided fundamental insights into albumin and hemoglobin's modeling. Lo.G., F.Z., T.L. and M.B. analyzed the data. Lo.G., T.L., F.Z., M.B., F.D., and E.P. drafted the manuscript. G.d.S. and A.d.M. formulated Figures 1 and S1. All authors revised the manuscript for important intellectual content and approved the final version to be submitted.

FIGURE LEGENDS

Figure 1. Changes in SID at varying pH

This figure depicts the predicted increase in Z_{pH} on albumin (heart shaped, upper part of the figure) and hemoglobin (inside a schematic red cell, lower part of the figure) when pH decreases from 7.8 to 6.8. The hypothesized effect of pH-induced changes in Z_{pH} on SID is also highlighted: the increase in albumin Z_{pH} is associated with release of bound calcium, and increased binding of chloride. Concomitantly, the increase in hemoglobin Z_{pH} drives chloride and water into red cells. Both phenomena determine an increase in SID. Based on previously published experiments (14, 17), we hypothesize that the overall change in SID to be expected for a given change in pH in whole-blood, equals the predictable change in albumin and hemoglobin's Z_{pH}. Implications of such hypothesis are discussed in the text. Note that, for the sake of simplicity, the figure neglects potassium and magnesium, whose pH-dependence is quantitatively less important than chloride, calcium, and sodium. Chloride binding to hemoglobin is also not shown since irrelevant to this paper. Albumin and hemoglobin were drawn using UCSF ChimeraX package (48).

Figure 2. Measured vs expected SID during respiratory acidosis (Experiment 1)

The figure displays mean values of measured and expected SID at every equilibrated CO_2 (on the left) and their agreement through a Bland-Altman plot (on the right) in isolated plasma (Panel A) and whole-blood (Panel B) of healthy subjects and septic patients. The step with 5% equilibrated CO_2 (*i.e.*, the baseline step) was not considered in the Bland-Altman analysis, as the measured and expected SID are equal by definition.

Figure 3. Measured vs expected SID during respiratory acidosis (Experiment 2)

On the left, mean values of measured and expected SID at every equilibrated CO_2 in non-diluted and diluted samples. On the right, their agreement through a Bland-Altman plot.

The step with 12% equilibrated CO_2 (*i.e.*, the baseline steps) was not considered in the Bland-Altman analyses, as the measured and expected SID are equal by definition.

Figure 4. Measured vs expected SID during respiratory acidosis (Experiment 3)

On the left, mean values of measured and expected SID at every equilibrated CO_2 in the control samples (*i.e.*, with no added strong acid). The expected SID was calculated either from albumin and hemoglobin's titrable charges (SID_{exp}) or from patients' specific whole-blood buffer value β $SID_{exp(\beta)}$. On the right, the agreement between SID and SID_{exp}, and between SID and $SID_{exp(\beta)}$ is displayed through a Bland-Altman plot. The step with the PCO_2 closest to 40 mmHg (*i.e.*, the baseline step) was not considered in the Bland-Altman analyses, as the measured and expected SID are equal by definition.

Figure 5. BE, SID, and SID_{wb} during metabolic and mixed acidosis (Experiment 3)

This figure displays changes in base excess, plasma SID and whole-blood SID from baseline to samples with added lactate or chloride. Mean changes are displayed on the left, Bland-Altman analysis on the right. In Panel A, all samples are at constant equilibrated CO_2 (metabolic acidosis), while in Panel B samples with added lactate or chloride are at any equilibrated CO_2 between 2 and 20% (mixed acidosis). The control sample with the PCO_2 closest to 40 mmHg (*i.e.*, the baseline step) was not considered in the Bland-Altman analysis, as all Δ are referred to baseline by definition.

Figure 6. Fencl-Stewart equation vs our simplified model applied to mixed acidosis

Data refer to whole-blood of one of the healthy subjects from Experiment 3 after addition of hydrochloric acid (~15 mEq/L) and equilibration with ~ 15% CO_2. As shown, ignoring electrolytes redistribution, the Fencl-Stewart equation underestimates the effect of strong ions on BE, erroneously implying the presence of unmeasured ions.

REFERENCES

1. **Morgan TJ**, **Clark C**, **Endre ZH**. Accuracy of base excess—An in vitro evaluation of the Van Slyke equation: *Critical Care Medicine* 28: 2932–2936, 2000. doi: 10.1097/00003246-200008000-00041.

2. **Andersen OS**. The pH-log pCO2 acid-base nomogram revised. *Scandinavian Journal of Clinical and Laboratory Investigation* 14: 598–604, 1962. doi: 10.1080/00365516209051290.

3. **Singer RB**, **Hastings AB**. An improved clinical method for the estimation of disturbances of the acid-base balance of human blood. *Medicine (Baltimore)* 27: 223–242, 1948. doi: 10.1097/00005792-194805000-00003.

4. **Berend K**. Diagnostic Use of Base Excess in Acid–Base Disorders. *N Engl J Med* 378: 1419–1428, 2018. doi: 10.1056/NEJMra1711860.

5. **Story DA**. Acid–Base Analysis in the Operating Room: A Bedside Stewart Approach. *Anesthesiology* 139: 860–867, 2023. doi: 10.1097/ALN.0000000000004712.

6. **Gilfix BM**, **Bique M**, **Magder S**. A physical chemical approach to the analysis of acid-base balance in the clinical setting. *Journal of Critical Care* 8: 187–197, 1993. doi: 10.1016/0883-9441(93)90001-2.

7. **Balasubramanyan N**, **Havens PL**, **Hoffman GM**. Unmeasured anions identified by the Fencl-Stewart method predict mortality better than base excess, anion gap, and lactate in patients in the pediatric intensive care unit. *Critical Care Medicine* 27: 1577, 1999. doi: 10.1097/00003246-199908000-00030.

8. **Fencl V**, **Jabor A**, **Kazda A**, **Figge J**. Diagnosis of Metabolic Acid–Base Disturbances in Critically Ill Patients. *Am J Respir Crit Care Med* 162: 2246–2251, 2000. doi: 10.1164/ajrccm.162.6.9904099.

9. **Story DA**, **Morimatsu H**, **Bellomo R**. Strong ions, weak acids and base excess: a simplified Fencl–Stewart approach to clinical acid–base disorders † †Presented in part at the Australian and New Zealand College of Anaesthetists Annual Scientific Meeting, May 12, 2002, Brisbane, Australia. *British Journal of Anaesthesia* 92: 54–60, 2004. doi: 10.1093/bja/aeh018.

10. **Morgan TJ**. The Stewart Approach – One Clinician's Perspective. *Clin Biochem Rev* 30: 41-54, 2009.

11. **Wolf MB**, **DeLand EC**. A comprehensive, computer-model-based approach for diagnosis and treatment of complex acid–base disorders in critically-ill patients. *J Clin Monit Comput* 25: 353–364, 2011. doi: 10.1007/s10877-011-9320-2.

12. **Stewart PA**. How to understand acid-based balance*:* A Quantitative Acid-Base Primer for Biology and Medicine. New York, Elsevier, 1981.

13. **Agrafiotis M**. Strong ion reserve: a viewpoint on acid base equilibria and buffering. *Eur J Appl Physiol* 111: 1951–1954, 2011. doi: 10.1007/s00421-010-1803-1.

14. **Fogh-Andersen N**, **Bjerrum PJ**, **Siggaard-Andersen O**. Ionic binding, net charge, and Donnan effect of human serum albumin as a function of pH. *Clinical Chemistry* 39: 48–52, 1993. doi: 10.1093/clinchem/39.1.48.

15. **Van Leeuwen AM**. Net cation equivalency ('base binding power') of the plasma proteins. *Acta Med Scand* 176: SUPPL 422: 1+, 1964.

16. **Funder J**, **Wieth JO**. Chloride and Hydrogen Ion Distribution between Human Red Cells and Plasma. *Acta Physiologica Scandinavica* 68: 234–245, 1966. doi: 10.1111/j.1748-1716.1966.tb03423.x.

17. **Dalmark M**. Chloride and water distribution in human red cells. *The Journal of Physiology* 250: 65–84, 1975. doi: 10.1113/jphysiol.1975.sp011043.

18. **Langer T**, **Brusatori S**, **Carlesso E**, **Zadek F**, **Brambilla P**, **Ferraris Fusarini C**, **Duska F**, **Caironi P**, **Gattinoni L**, **Fasano M**, **Lualdi M**, **Alberio T**, **Zanella A**, **Pesenti A**, **Grasselli G**. Low noncarbonic buffer power amplifies acute respiratory acid-base disorders in patients with sepsis: an in vitro study. *Journal of Applied Physiology* 131: 464–473, 2021. doi: 10.1152/japplphysiol.00787.2020.

19. **Langer T**, **Scotti E**, **Carlesso E**, **Protti A**, **Zani L**, **Chierichetti M**, **Caironi P**, **Gattinoni L**. Electrolyte shifts across the artificial lung in patients on extracorporeal membrane oxygenation: Interdependence between partial pressure of carbon dioxide and strong ion difference. *Journal of Critical Care* 30: 2–6, 2015. doi: 10.1016/j.jcrc.2014.09.013.

20. **Zadek F**, **Danieli A**, **Brusatori S**, **Giosa L**, **Krbec M**, **Antolini L**, **Fumagalli R**, **Langer T**. Combining the Physical–Chemical Approach with Standard Base Excess to Understand the Compensation of Respiratory Acid–Base Derangements: An Individual Participant Meta-analysis Approach to Data from Multiple Canine and Human Experiments. *Anesthesiology* 140: 116-125, 2024. doi: 10.1097/ALN.0000000000004751.

21. **Böning D**, **Klarholz C**, **Himmelsbach B**, **Hütler M**, **Maassen N**. Causes of differences in exercise-induced changes of base excess and blood lactate. *Eur J Appl Physiol* 99: 163–171, 2006. doi: 10.1007/s00421-006-0328-0.

22. **Peters JP**, **Tulin M**, **Danowski TS**, **Hald PM**. The distribution and movements of carbon dioxide and chloride between cells and serum of oxygenated human blood. *American Journal of Physiology-Legacy Content* 148: 568–581, 1947. doi: 10.1152/ajplegacy.1947.148.3.568.

23. **Madias NE**, **Homer SM**, **Johns CA**, **Cohen JJ**. Hypochloremia as a consequence of anion gap metabolic acidosis. *The Journal of Laboratory and Clinical Medicine* 104: 15–23, 1984. doi: 10.5555/uri:pii:0022214384901276.

24. **Wooten EW**. Calculation of physiological acid-base parameters in multicompartment systems with application to human blood. *Journal of Applied Physiology* 95: 2333–2344, 2003. doi: 10.1152/japplphysiol.00560.2003.

25. **Watson PD**. Modeling the effects of proteins on pH in plasma. *Journal of Applied Physiology* 86: 1421–1427, 1999. doi: 10.1152/jappl.1999.86.4.1421.

26. **Siggaard-Andersen O**. The acid-base status of the blood. Williams & Wilkins Company, 1964

27. **Krbec M**, **Waldauf P**, **Zadek F**, **Brusatori S**, **Zanella A**, **Duška F**, **Langer T**. Non-carbonic buffer power of whole blood is increased in experimental metabolic acidosis: An in-vitro study. *Frontiers in Physiology* 13:1009378, 2022. doi: 10.3389/fphys.2022.1009378

28. **Figge J**, **Mydosh T**, **Fencl V**. Serum proteins and acid-base equilibria: a follow-up. *J Lab Clin Med* 120: 713–719, 1992.

29. **Tanford C**, **Nozaki Y**. Titration of the Histidyl and α-Amino Groups of Hemoglobin. *Journal of Biological Chemistry* 241: 2832–2839, 1966. doi: 10.1016/S0021-9258(18)96539-7.

30. **Reeves RB**. Temperature-induced changes in blood acid-base status: pH and PCO2 in a binary buffer. *J Appl Physiol* 40: 752–761, 1976. doi: 10.1152/jappl.1976.40.5.752.

31. **Lang W**, **Zander R**. The Accuracy of Calculated Base Excess in Blood. *Clinical Chemistry and Laboratory Medicine* 40, 2002. doi: 10.1515/CCLM.2002.065.

32. **Clinical and Laboratory Standards Institute.** Blood gas & pH analysis & related measurements. Wayne, PA: CLSI. Approved Guideline--Second Edition, C46A2, 2009

33. **Story DA**, **Poustie S**, **Bellomo R**. Estimating unmeasured anions in critically ill patients: Anion-gap, base-deficit, and strong-ion-gap. *Anaesthesia* 57: 1109–1114, 2002. doi: 10.1046/j.1365-2044.2002.02782_2.x.

34. **Staempfli HR**, **Constable PD**. Experimental determination of net protein charge and Atot and Ka of nonvolatile buffers in human plasma. *Journal of Applied Physiology* 95: 620–630, 2003. doi: 10.1152/japplphysiol.00100.2003.

35. **Apple FS**, **Koch DD**, **Graves S**, **Ladenson JH**. Relationship between direct-potentiometric and flame-photometric measurement of sodium in blood. *Clinical Chemistry* 28: 1931–1935, 1982. doi: 10.1093/clinchem/28.9.1931.

36. **Van Slyke DD**, **Wu H**, **McLean FC**. Studies of gas and electrolyte equilibria in the blood: v. Factors controlling the electrolyte and water distribution in the blood. *Journal of Biological Chemistry* 56: 765–849, 1923. doi: 10.1016/S0021-9258(18)85558-2.

37. **Reeves RB**. An imidazole alphastat hypothesis for vertebrate acid-base regulation: tissue carbon dioxide content and body temperature in bullfrogs. *Respir Physiol* 14: 219-361, 972 Mar. doi: 10.1016/0034-5687(72)90030-8.

38. **Reeves RB**. Temperature-induced changes in blood acid-base status: Donnan rCl and red cell volume. *Journal of Applied Physiology* 40: 762–767, 1976. doi: 10.1152/jappl.1976.40.5.762.

39. **Böning D**, **Maassen N**. Blood osmolality in vitro: dependence on PCO2, lactic acid concentration, and O2 saturation. *J Appl Physiol Respir Environ Exerc Physiol* 54: 118–122, 1983. doi: 10.1152/jappl.1983.54.1.118.

40. **Van Slyke DD**. On the measurement of buffer values and on the relationship of buffer value to the dissociation constant of the buffer and the concentration and reaction of the buffer solution. *Journal of Biological Chemistry* 52: 525–570, 1922. doi: 10.1016/S0021-9258(18)85845-8.

41. **Böning D**, **Klarholz C**, **Himmelsbach B**, **Hütler M**, **Maassen N**. Extracellular bicarbonate and non-bicarbonate buffering against lactic acid during and after exercise. *Eur J Appl Physiol* 100: 457–467, 2007. doi: 10.1007/s00421-007-0453-4.

42. **Böning D**, **Rojas J**, **Serrato M**, **Reyes O**, **Coy L**, **Mora M**. Extracellular pH defense against lactic acid in untrained and trained altitude residents. *Eur J Appl Physiol* 103: 127–137, 2008. doi: 10.1007/s00421-008-0675-0.

43. **Fitzsimons E**, **Sendroy J**. Distribution of Electrolytes in Human Blood. *Journal of Biological Chemistry* 236: 1595–1601, 1961. doi: 10.1016/S0021-9258(18)64218-8.

44. **Johnson RE**, **Edwards HT**, **Dill DB**, **Wilson JW**. Blood as a physicochemical system: XIII. The distribution of lactate. *Journal of Biological Chemistry* 157: 461–473, 1945. doi: 10.1016/S0021-9258(18)51082-6.

45. **Story DA**, **Poustie S**, **Bellomo R**. Comparison of Three Methods to Estimate Plasma Bicarbonate in Critically Ill Patients: Henderson-Hasselbalch, Enzymatic, and Strong-Ion-Gap. *Anaesth Intensive Care* 29: 585–590, 2001. doi: 10.1177/0310057X0102900603.

46. **Deuticke B**. Anion permeability of the red blood cell. *Naturwissenschaften* 57: 172–179, 1970. doi: 10.1007/BF00592968.

47. **Schlichtig R**, **Grogono AW**, **Severinghaus JW**. Human PaCO2 and standard base excess compensation for acid-base imbalance. *Crit Care Med* 26: 1173–1179, 1998. doi: 10.1097/00003246-199807000-00015.

48. **Pettersen EF**, **Goddard TD**, **Huang CC**, **Meng EC**, **Couch GS**, **Croll TI**, **Morris JH**, **Ferrin TE**. UCSF ChimeraX: Structure visualization for researchers, educators, and developers. *Protein Science* 30: 70–82, 2021. doi: 10.1002/pro.3943.

Quantifying pH-induced changes in plasma SID during experimental acidosis: clinical implications for BE interpretation

Methods

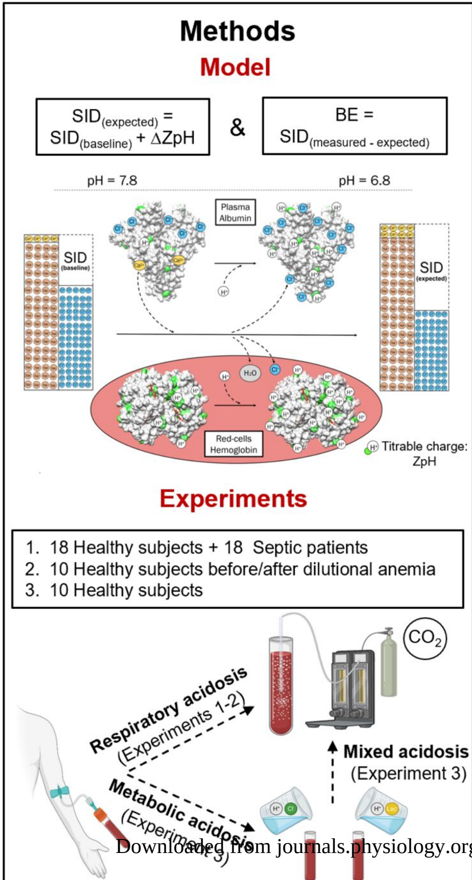

Outcomes

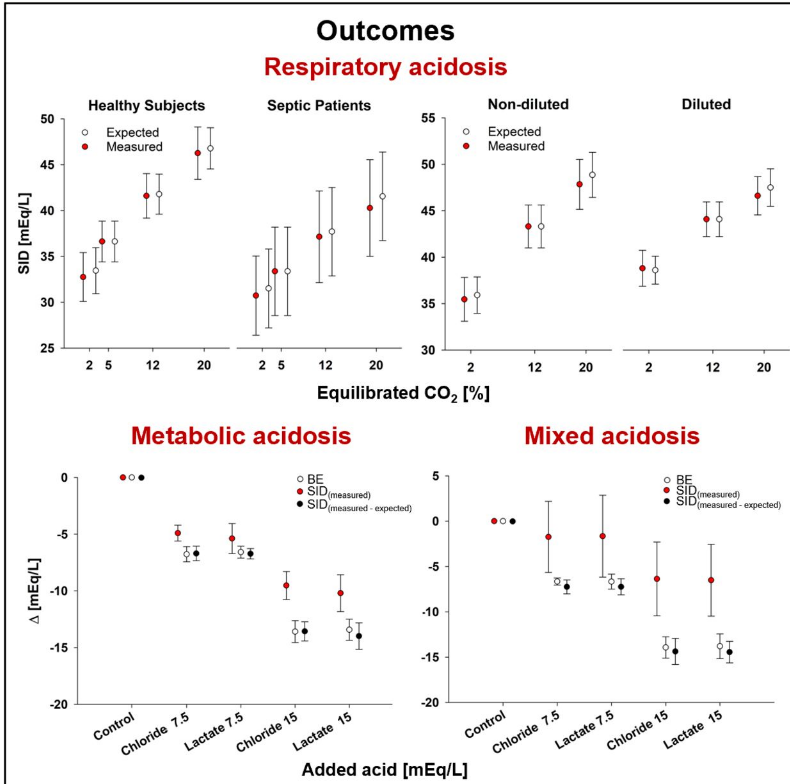

Conclusions

1. pH-induced changes in plasma SID are predictable from albumin and hemoglobin's charges.
2. BE reflects only changes in plasma SID that are not *expected* from electrolytes redistribution.

Table 1. Whole-blood CO_2 tonometry in Experiment 1

	Healthy Subjects (n=18)				Septic Patients (n=18)			
Variable	**2%**	**5%**	**12%**	**20%**	**2%**	**5%**	**12%**	**20%**
PCO_2	18.2 ±2.1	32.1 ±3.4	68.3 ±4.9	124.4 ±10.2	18.3 ±2.0	29.6 ±2.7	67.2 ±5.7	122.7 ±11.0
pH	7.61 ±0.04	7.46 ±0.03	7.24 ±0.03	7.07 ±0.03	7.56 ±0.11	7.41 ±0.10	7.17 ±0.09	6.98 ±0.09
HCO_3^-	18.0 ±1.2	22.8 ±1.8	29.6 ±1.6	35.7 ±2.0	16.8 ±4.3	19.5 ±5.2	25.1 ±5.4	29.7 ±5.6
Na^+	137.3 ±2.1	138.9 ±2.0	140.7 ±2.1	142.7 ±2.1	138.7 ±5.1	138.9 ±5.1	140.4 ±5.2	141.7 ±5.3
K^+	4.23 ±0.32	4.25 ±0.36	4.32 ±0.28	4.48 ±0.39	4.35 ±0.53	4.32 ±0.57	4.48 ±0.70	4.57 ±0.58
Ca^{++}	1.09 ±0.05	1.17 ±0.05	1.28 ±0.05	1.36 ±0.06	1.05 ±0.07	1.10 ±0.08	1.17 ±0.08	1.22 ±0.09
Mg^{++}	2.10 ±0.14	2.11 ±0.15	2.11 ±0.15	2.11 ±0.15	2.00 ±0.41	2.05 ±0.45	2.05 ±0.45	2.05 ±0.45
Cl^-	111 ±2	109 ±2	106 ±2	104 ±2	112 ±4	110 ±4	108 ±4	107 ±4
Lac^-	1.9 ±0.5	1.7 ±0.6	1.7 ±0.5	1.7 ±0.5	3.8 ±2.7	3.6 ±2.8	3.6 ±2.7	3.5 ±2.7
SID	32.8 ±2.7	36.6 ±2.2	41.6 ±2.4	46.3 ±2.9	30.7 ±4.3	33.4 ±4.8	37.1 ±5.0	40.3 ±5.3
$Z_{pH\ (Alb)}$	1.4 ±0.1	1.9 ±0.1	2.8 ±0.2	3.7 ±0.2	1.0 ±0.2	1.4 ±0.3	2.1 ±0.4	2.7 ±0.5
$Z_{pH\ (Hb)}$	11.2 ±1.1	13.7 ±1.1	17.9 ±1.2	22.9 ±1.5	8.7 ±1.4	10.7 ±1.4	14.3 ±1.5	17.4 ±1.7
SID_{exp}	33.5 ±2.5	36.6 ±2.2	41.8 ±2.2	46.8 ±2.3	31.5 ±4.3	33.4 ±4.8	37.7 ±4.8	41.6 ±4.8

Table 2. Whole-blood CO_2 tonometry in Experiment 2

	Diluted (n=10)			Undiluted (n=10)		
Variable	**2%**	**12%**	**20%**	**2%**	**12%**	**20%**
PCO_2	18.6 ±4.8	66.9 ±3.7	118.4 ±9.3	19.9 ±3.3	64.2 ±5.3	121.2 ±8.8
pH	7.69 ±0.08	7.25 ±0.03	7.06 ±0.04	7.60 ±0.05	7.27 ±0.03	7.08 ±0.03
HCO_3^-	22.2 ±2.3	29.6 ±2.3	33.5 ±2.3	19.6 ±2.1	29.8 ±2.2	36.1 ±2.7
Na^+	139.7 ±1.2	141.6 ±1.2	142.6 ±1.3	139.2 ±1.4	142.0 ±1.6	143.8 ±1.6
K^+	3.97 ±0.23	3.98 ±0.28	4.06 ±0.25	4.10 ±0.23	4.12 ±0.27	4.22 ±0.23
Ca^{++}	1.03 ±0.03	1.28 ±0.03	1.38 ±0.02	1.09 ±0.03	1.28 ±0.03	1.37 ±0.03
Mg^{++}	2.05 ±0.12	2.07 ±0.13	2.09 ±0.14	2.02 ±0.10	2.06 ±0.10	2.10 ±0.11
Cl^-	107 ±2	104 ±2	103 ±2	110 ±2	105 ±2	103 ±2
Lac^-	1.5 ±0.3	1.4 ±0.2	1.3 ±0.2	1.9 ±0.4	1.7 ±0.4	1.6 ±0.4
SID	38.8 ±1.9	44.1 ±1.9	46.6 ±2.1	35.5 ±2.4	43.3 ±2.3	47.8 ±2.7
$Z_{pH\ (Alb)}$	1.2 ±0.2	2.9 ±0.1	4.0 ±0.3	1.5 ±0.2	2.8 ±0.2	3.9 ±0.3
$Z_{pH\ (Hb)}$	4.8 ±0.7	8.7 ±1.1	11.0 ±1.3	11.0 ±1.3	17.1 ±1.9	21.5 ±2.4
SID_{exp}	38.6 ±1.5	44.1 ±1.9	47.5 ±2.0	35.9 ±2.0	43.3 ±2.3	48.9 ±2.4

Table 3. Metabolic acidosis at constant equilibrated CO_2 in Experiment 3

Metabolic Acidosis (n=10)					
Variable	**Ctr**	**Lac 7.5**	**Cl 7.5**	**Lac 15**	**Cl 15**
PCO_2	39.9 ± 3.2	39.4 ± 3.5	40.9 ± 2.9	40.4 ± 1.8	40.5 ± 2.1
pH	7.40 ± 0.03	7.30 ± 0.02	7.29 ± 0.03	7.18 ± 0.04	7.18 ± 0.04
HCO_3^-	24.8 ± 1.4	19.6 ± 1.8	19.8 ± 1.7	15.3 ± 1.2	15.2 ± 1.2
Na^+	142.9 ± 1.9	143.5 ± 1.9	144.6 ± 1.4	144.6 ± 1.4	146.2 ± 1.7
K^+	4.0 ± 0.3	4.0 ± 0.3	4.0 ± 0.3	4.0 ± 0.3	4.2 ± 0.2
Ca^{++}	1.1 ± 0.0	1.2 ± 0.0	1.2 ± 0.0	1.2 ± 0.0	1.3 ± 0.0
Mg^{++}	2.0 ± 0.1	2.0 ± 0.1	2.0 ± 0.1	2.0 ± 0.1	2.0 ± 0.1
Cl^-	106.4 ± 1.2	105.3 ± 1.1	113.2 ± 1.2	104.2 ± 0.9	119.9 ± 1.4
Lac^-	1.6 ± 0.3	8.7 ± 0.4	1.6 ± 0.4	15.8 ± 0.7	1.5 ± 0.3
SID	42.9 ± 2.5	37.5 ± 2.5	38.0 ± 2.4	32.7 ± 2.0	33.3 ± 2.7
β	28.5 ± 2.8	30.6 ± 2.5	31.1 ± 2.6	33.1 ± 2.9	33.7 ± 2.8
BE	0.0 ± 1.5	-6.6 ± 1.7	-6.8 ± 1.8	-13.4 ± 2.2	-13.6 ± 2.1
∆SID	/	-5.4 ± 1.3	-4.9 ± 0.7	-10.2 ± 1.6	-9.5 ± 1.2
∆BE	/	-6.6 ± 0.5	-6.8 ± 0.7	-13.4 ± 0.9	-13.6 ± 1.0
ΔSID_{wb}	/	-6.7 ± 0.5	-6.7 ± 0.7	-14.0 ± 1.2	-13.5 ± 0.8

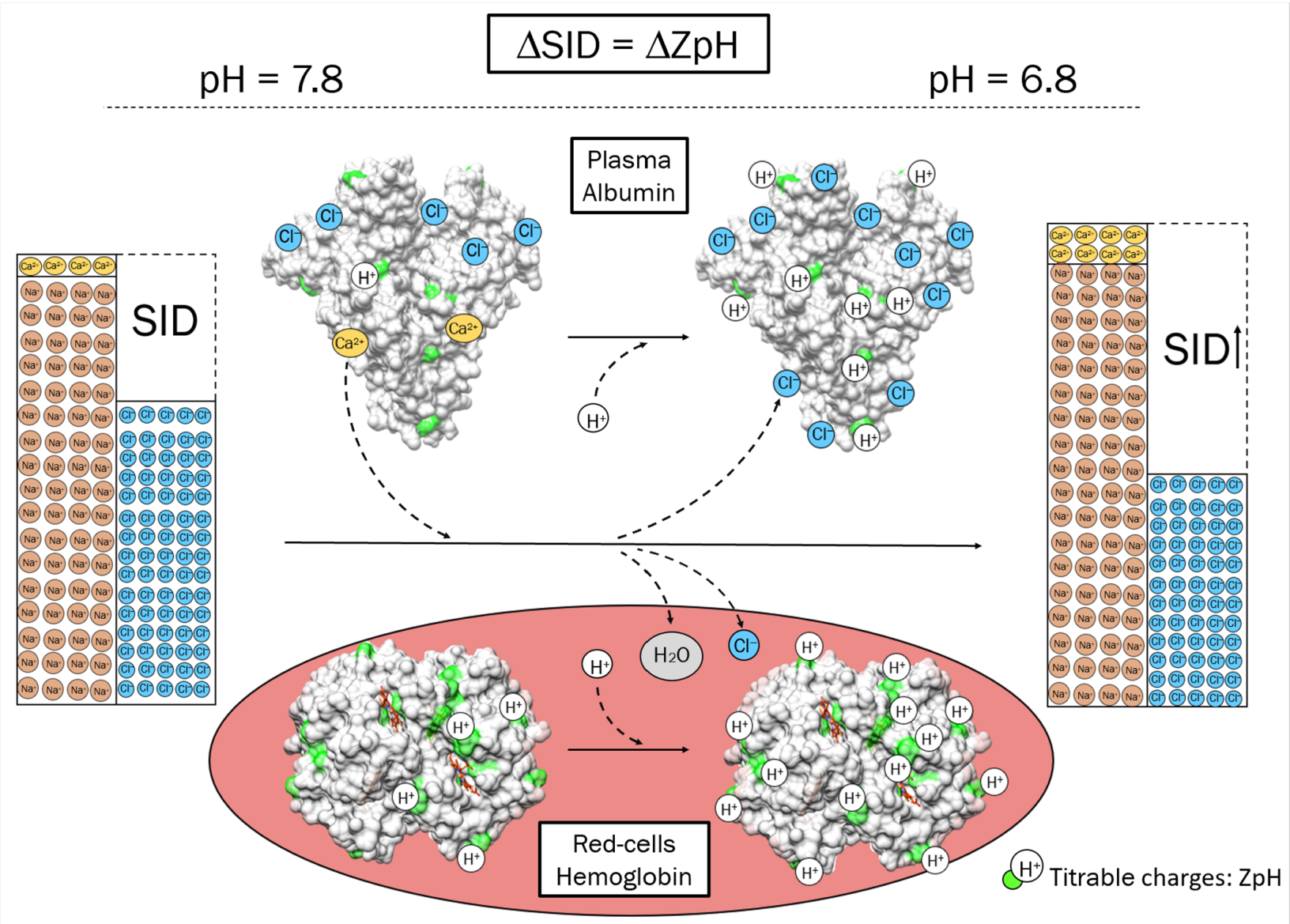

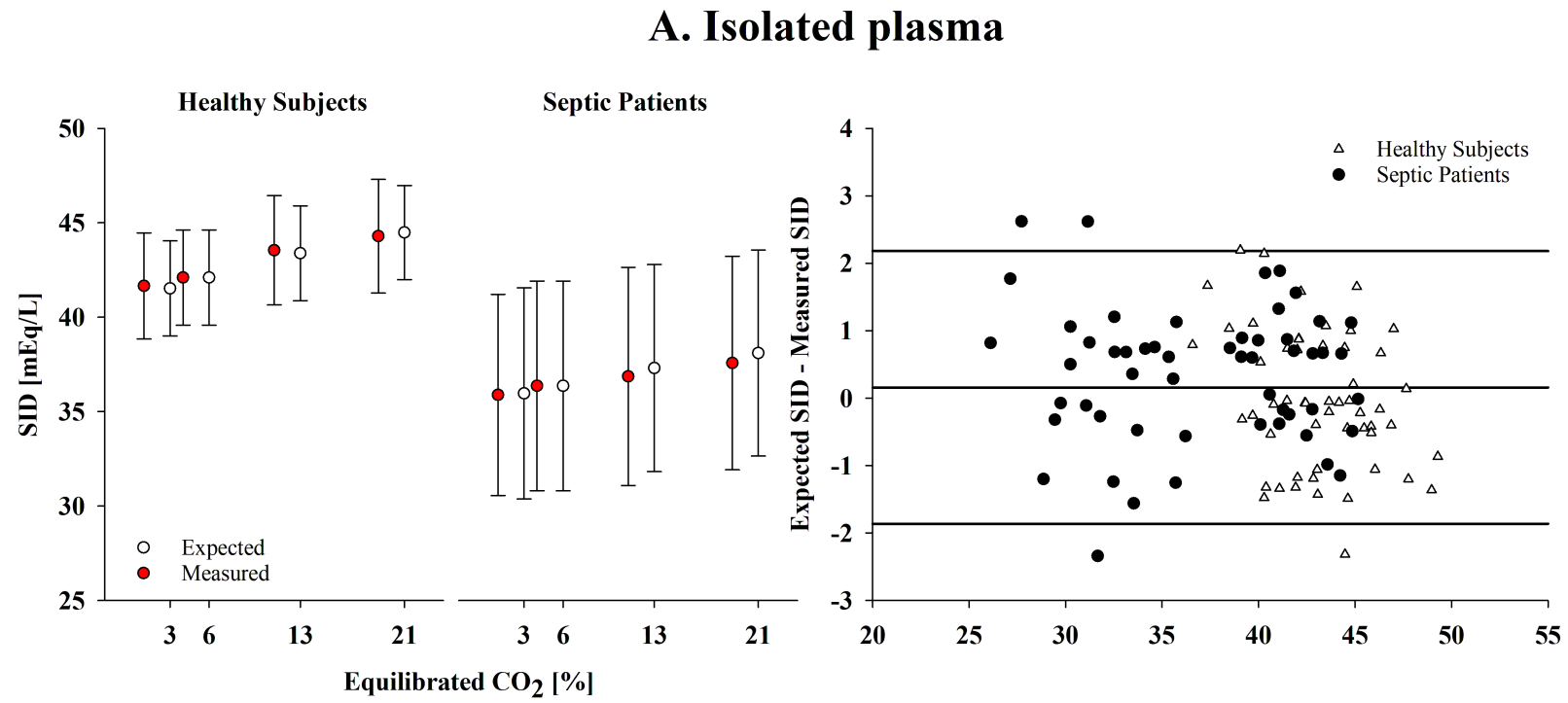

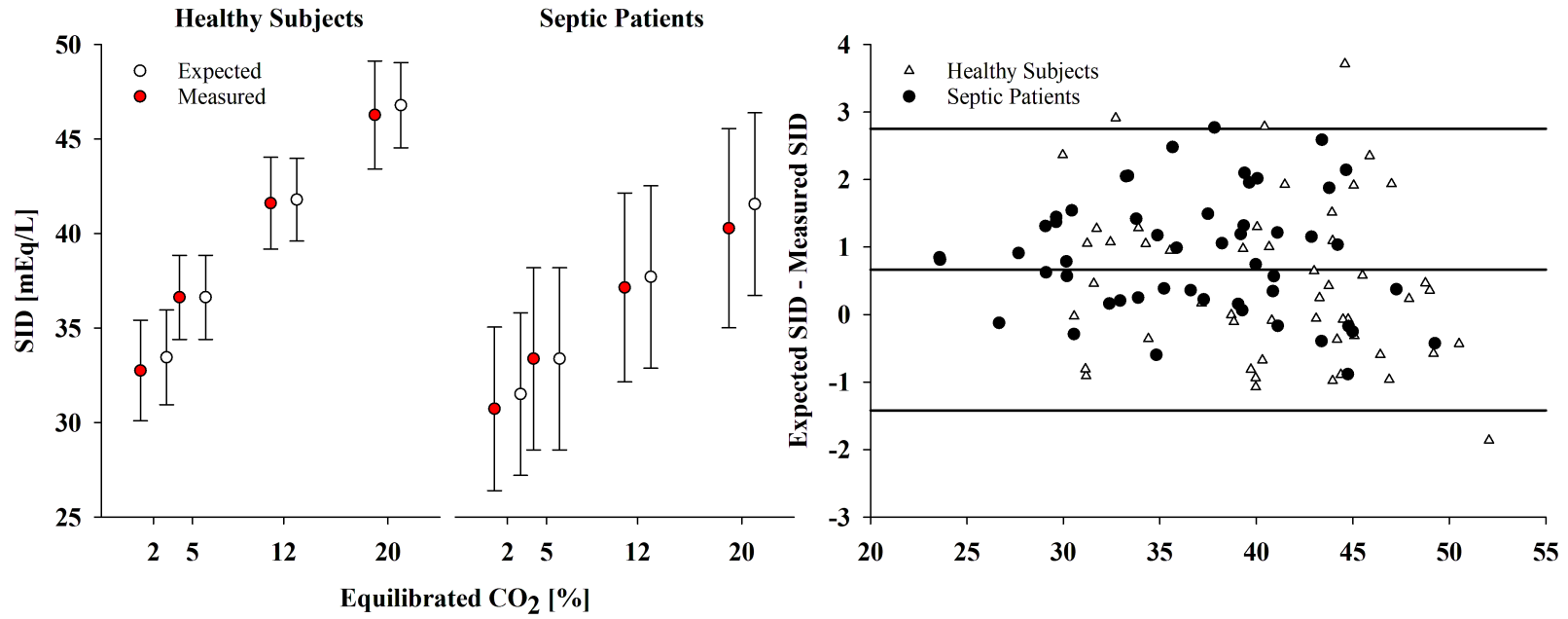

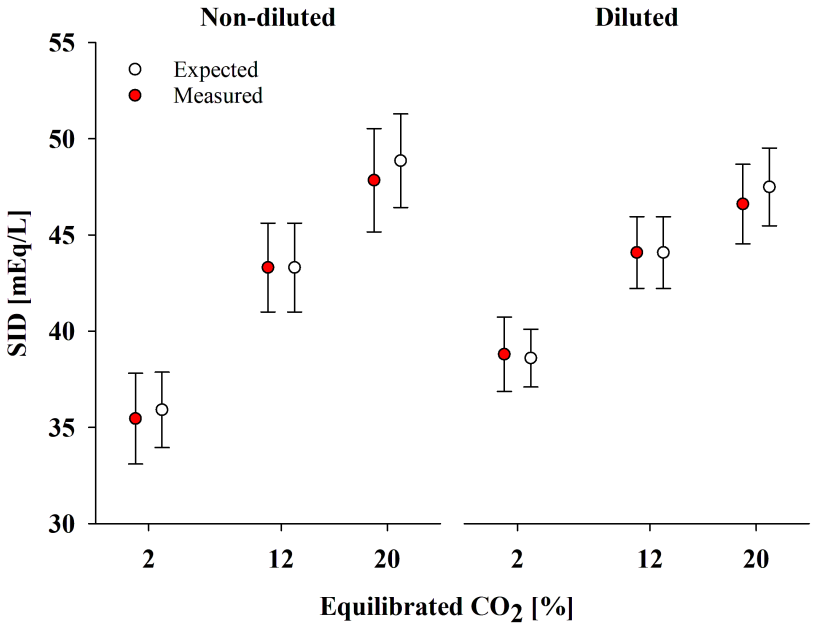

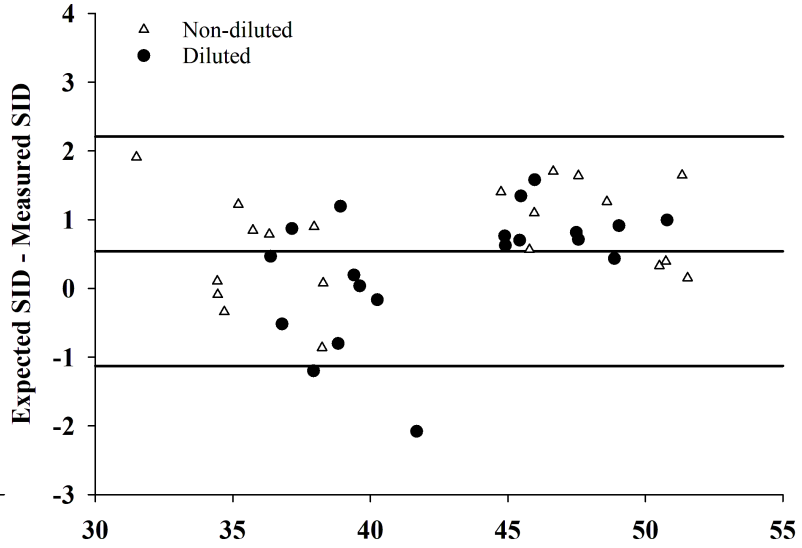

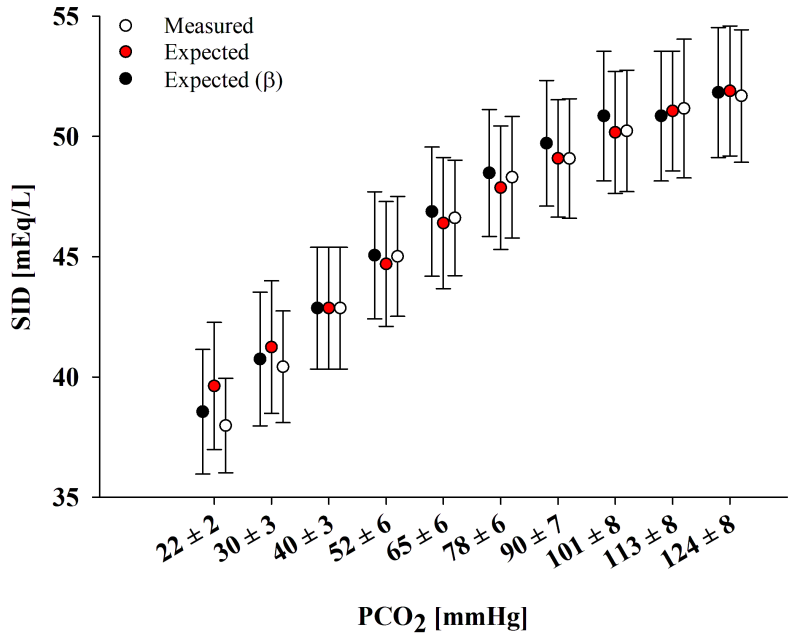

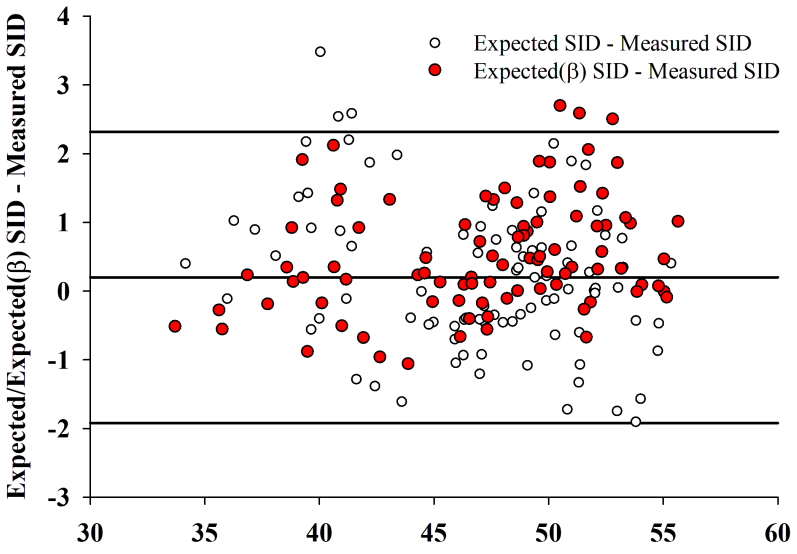

A. Metabolic acidosis

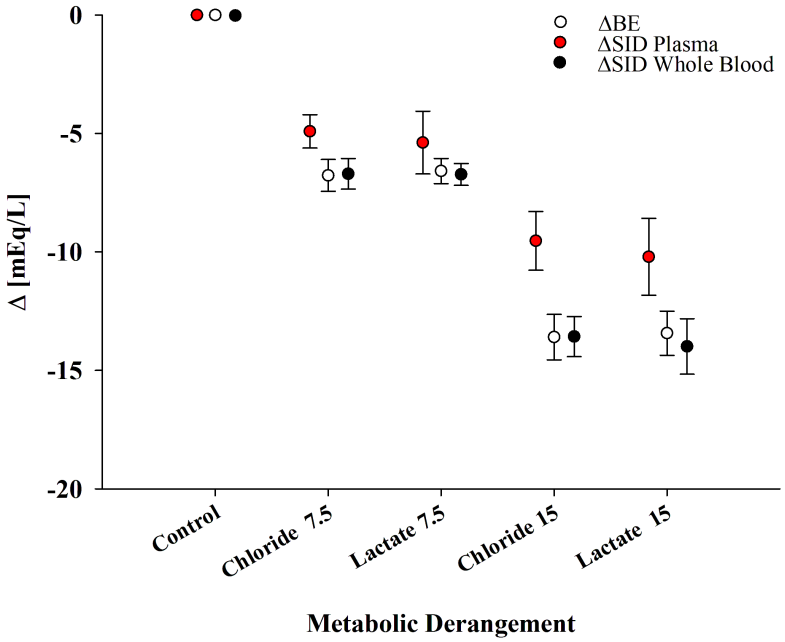

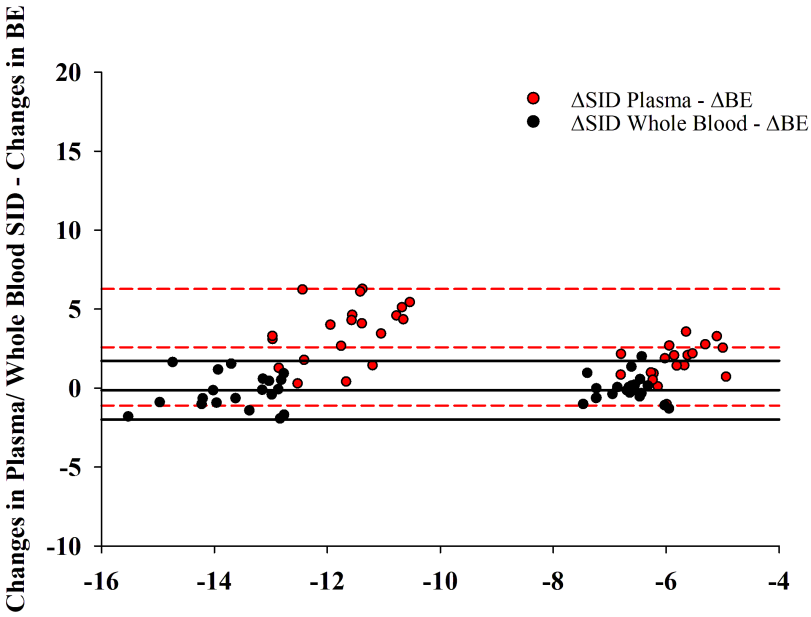

B. Mixed acidosis